JOURNAL OF SPACECRAFT AND ROCKETS
Vol. 37, No. 6, November–December 2000

Trajectories to Jupiter via Gravity Assists from Venus, Earth, and Mars

Anastassios E. Petropoulos,* James M. Longuski,† and Eugene P. Bonfiglio‡
Purdue University, West Lafayette, Indiana 47907-1282

Gravity-assist trajectories to Jupiter, launching between 1999 and 2031, are identified using patched-conic techniques. The classical trajectories, such as the Venus–Earth–Earth gravity assist, and many less conventional paths, such as Venus–Mars–Venus–Earth, are examined. Flight times of up to about seven years are considered. The ΔV-optimized results confirm that Venus–Earth–Earth is the most effective gravity-assist trajectory type, with launch opportunities occurring almost every year and launch vis viva for ballistic trajectories as low as 9 km^2/s^2. If the Earth is excluded as a flyby body, Venus–Venus–Venus gravity assists are typically the best option, with launch vis viva for ballistic trajectories as low as 30 km^2/s^2, although in some years nonconventional paths are better, such as a ballistic Venus–Mars–Venus–Venus trajectory in 2012, with a launch vis viva of 16 km^2/s^2. Nonconventional paths, such as Venus–Mars–Venus–Earth with a 3.7-year flight-time trajectory in 2021, can occasionally decrease the time of flight significantly, at very minor ΔV cost, when compared with the classical types.

Introduction

THE principle of gravity assist has a rich and interesting history, and numerous researchers have contributed to its theory and application. (See Refs. 1–25 for a small sampling of the literature.) In this paper we identify gravity-assist trajectories via Venus, Earth, and Mars to Jupiter during a three-decade launch period from 1999 to 2031. We are interested in low-launch-energy trajectories with low total ΔV (i.e., magnitude of the velocity changes effected by thrusters, modeled impulsively) and with reasonable times of flight (less than about seven years). We examine 25 different sequences of gravity-assist bodies with the automated Satellite Tour Design Program[16–21] (STOUR), which is capable of finding all patched-conic, gravity-assist trajectories for a given set of launch dates and launch V_∞ (hyperbolic excess speeds). In addition, the automated STOUR can compute trajectories with ΔV applied in three different modes: powered flyby,[19] broken plane,[19] and V_∞-leveraging.[21,25] For selected cases we find the ΔV-optimal solutions using the Jet Propulsion Laboratory's Mission Design and Analysis Software[22] (MIDAS). Because we are considering up to four gravity assists with three of the inner planets, there are 120 possible paths (or combinations). Although STOUR is a very powerful tool, it takes several days (on a typical computer workstation) to assess one path for a three-decade launch period. Thus it is impractical to merely grind through all possible combinations, and so, as is often the case, engineering judgment and analysis are required. We find the simple analytic techniques developed by Hollenbeck[23] very helpful in predicting the potential performance of paths involving only combinations of Venus and Earth gravity assists. Further refinements of these techniques are given by Sims[24] and Sims et al.[25] We extend this concept to include up to four gravity assists, giving deep insight into which paths are likely to be effective. Perhaps more importantly, our technique indicates which paths are ineffective, allowing us to reject a large fraction of paths at an early stage of the analysis. We call the problem of selection "pathfinding"; it is the central issue of multiple-gravity-assist mission design.

Classical Paths

Certain highly effective trajectory types have been well known and commonly used in mission planning, thus meriting the name "classical." Specifically, in this paper the classical trajectories will be taken as Delta-V–Earth gravity assist (ΔV–EGA), Venus–Earth gravity assist (VEGA), Venus–Earth–Earth gravity assist (VEEGA), V^2, and V^3, where V^n denotes n Venus gravity assists after Earth launch.

The exterior ΔV-EGA is a V_∞-leveraging trajectory[25] in which a maneuver (ΔV) is performed near aphelion after Earth launch, such that the spacecraft reencounters Earth with a higher V_∞ for the final gravity assist. The symmetric case, where the maneuver is performed near perihelion, is termed interior.

In the case of VEGA, VEEGA, and V^n trajectories to Jupiter, the disadvantage of launching into a lower-energy orbit to reach the first Venus encounter is more than offset by the benefit of a high V_∞ at a body that is almost as massive as the Earth. In fact, for typical launch V_∞, the V_∞ magnitude at Venus is so high that a single flyby of the planet cannot turn the V_∞ vector enough to reach Jupiter. A second flyby of Venus is also insufficient but can be adequately augmented with a maneuver during or after the flyby. A third Venus flyby can alleviate the need for the maneuver. The VEGAs and VEEGAs are more effective from an energy standpoint not only because Earth can provide slightly more V_∞ turning but also because after the Venus flyby we no longer need to maintain a perihelion distance as low as Venus's orbit. V_∞-leveraging can often be effectively incorporated into paths with repeated flybys of the same body.

A salient feature of the classical trajectories, which accounts for their common use, is the fact that launch opportunities occur relatively frequently: at least every two to three years, typically (when the planets realign), as is readily seen from the launch-date plots produced by STOUR. For example, Fig. 1 shows time of flight (TOF) vs launch date for low-launch-energy VEEGAs. Each numeral on the plot represents a trajectory with a certain launch energy (for example, a 4 within the plot axes corresponds to the fourth launch V_∞ in the VINF list near the top of the figure, 3.75 km/s; see Table 1 for further details). Although, given the large number of trajectories, the individual numerals (e.g., 1, 2, 3, and 4 in Fig. 1) are sometimes difficult to discern, because our objective at this point is to observe the overall trends, the readability of the numerals is of little concern. Specific trajectories can be chosen from a family by focusing on a smaller date range to make the numerals more discernible, if necessary. Another example of a launch-date plot is shown in Fig. 2 for V^3 trajectories with leveraging maneuvers between both Venus

Presented as Paper 98-4284 at the AIAA/AAS Astrodynamics Specialist Conference, Boston, MA, 10–12 August 1998; received 19 August 1999; revision received 1 March 2000; accepted for publication 13 March 2000.

*Ph.D. Candidate, School of Aeronautics and Astronautics. Member AIAA.

†Professor, School of Aeronautics and Astronautics. Associate Fellow AIAA.

‡M.S. Candidate, School of Aeronautics and Astronautics. currently Member of the Technical Staff, Navigation and Mission Design Section, Mail Stop 301-335, Jet Propulsion Laboratory, California Institute of Technology, 4800 Oak Grove Drive, Pasadena, CA 91109-8099. Student Member AIAA.

Table 1 Legend for launch-date plots

Variable	Description
PATH	Planets encountered, including launch and destination bodies, e.g., PATH: 3 2 3 3 5 is a VEEGA from Earth to Jupiter. Maneuvers represented by 0.
VINF	Launch V_∞ . Without maneuvers present, the numerals 1, 2, 3, 4, . . . on the plot represent the 1st, 2nd, 3rd, 4th,. . . V_∞ in the VINF list above the plot. For example, in Fig. 1 the numeral 3 on the plot denotes a V_∞ of 3.50 km/s. With maneuvers, only one launch V_∞ is shown, as in Fig. 2, where a 1 represents a ΔV between 0 and 1 km/s, a 2 represents 1–2 km/s, etc.
SEARCH EVENT NO.	Event in PATH for which data are plotted. For example, in Fig. 2, TOF to Jupiter is plotted because encounter with Jupiter is the 8th event in the PATH.
ALTMIN	Minimum flyby altitude permitted in the STOUR run.
SEARCH MIN. ALT.	Trajectories with flyby altitudes below this value are not included in the plot.
LAUNCH DATES SEARCHED	Launch-date range (YY/MM/DD) used in the STOUR run. For example, 99/1/1 means 1 Jan. 1999. The launch-date increment is also given, e.g., "by 5.0 days."
TFMAX	Maximum allowable time of flight in the STOUR run.

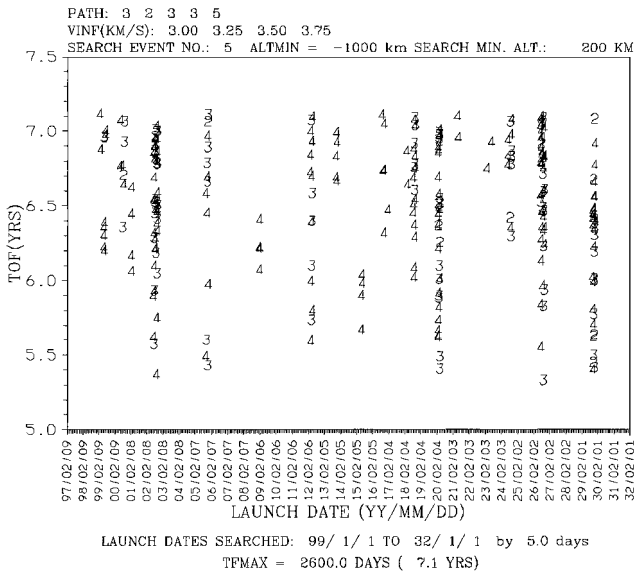

Fig. 1 Resonant and nonresonant, low-launch-energy VEEGAs with arrival V_∞ < 8 km/s.

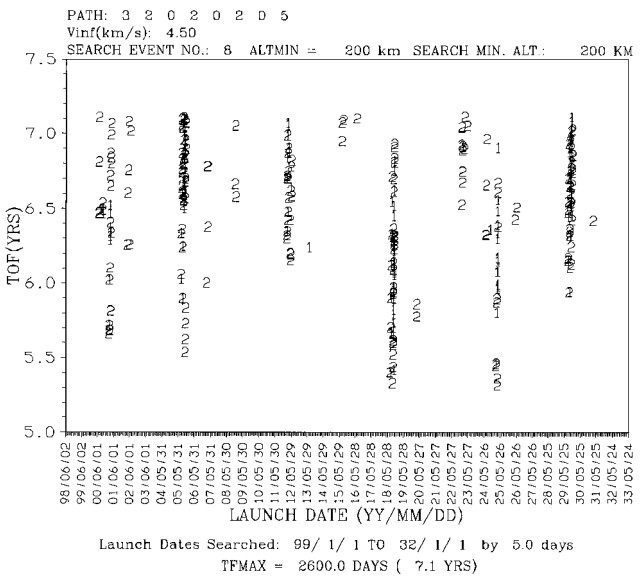

Fig. 2 V^3 trajectories with two V_∞ -leveraging maneuvers (combined $\Delta V \leq 1.25$ km/s).

pairs. In this case each numeral on the plot represents a certain total deep-space ΔV. Although the classical trajectories are frequently available, nonclassical trajectories must also be studied, not only to fill the gaps in the launch-date space but also to determine any instances where they are superior to the classical options.

Identification of Nonclassical Paths

There are several approaches one might take in determining which nonclassical paths may be effective. The first approach employed was to seek variations on the classical paths. One such variation uses a gravity assist at another planet to achieve a V_∞ -leveraging effect. This technique is used, for example, by Sims et al.[25] Thus we use such paths as VMV^2 and VEME, where Mars is the leveraging body. Another type of variation on classical paths is the simple addition of another gravity-assist body while outward bound for Jupiter. Examples include VEM and V^2E. (In fact, the Cassini spacecraft is using a Venus–Venus–Earth–Jupiter gravity assist to reach Saturn.) There is also the obvious insertion of a Mars flyby on a direct Earth-to-Jupiter trajectory. These variations may be used in combination, to yield such paths as VMVE. Another variation is the repetition of a classical type, as in VEVE. A more radical variation is the substitution of Mars for Venus, giving such paths as ME, ME^2, and M^2.

The natural concern in devising these paths is the frequency of launch opportunities. STOUR has been our workhorse in addressing this concern; we also discuss some specific cases in a later section. However, it should be noted that the frequency for a particular path is not always easily inferred: for example, there is no obvious reason why VMV^2 occurs far less frequently than VEME (for a maximum TOF of about seven years), yet this difference is what the STOUR results indicate.

Another approach to pathfinding is to simply list all possible combinations and judiciously rank the list. The restrictions on the paths considered (Venus, Earth, and Mars flybys with a limit of four flybys) leaves a complete list of 120 unique paths. Cutting the 120 paths down to a workable number requires intuition and experience. To aid our intuition, we created gravity assist potential (GAP) plots for each path. These plots assist in determining the maximum possible aphelion for a given path. For these plots we assume that the trajectories are ballistic (i.e., there are no deep-space maneuvers), the launch from Earth is always tangential, the planetary orbits are circular and coplanar, and there is no overturning. (That is, the V_∞ vector is turned as much as possible without turning past alignment with the velocity vector of the flyby planet.) For multiple flybys, such as VM^2V, the V_∞ vector is turned in a positive sense at the first Venus encounter (toward alignment with Venus's velocity vector) because the next planet in the path is outward (i.e., more distant from the sun). At the second planet, Mars, the V_∞ vector is turned in a negative sense (against alignment with Mars's velocity vector) because, although the next planet is the same (Mars), the planet after that (the last, Venus) is inward, and turning in this direction will tend to decrease perihelion. In other words, if the next different planet is inward, the V_∞ vector is turned negatively; if it is outward, the V_∞ vector is turned positively. If we did not turn the V_∞ vector negatively when heading inward (with respect to the sun), then, in a case like the VM^2V, the spacecraft would not be able to get back to Venus after the second Mars encounter. Of course, at the last planet in every path, the V_∞ vector is turned in a positive sense to maximize the final aphelion radius. Flyby altitudes as low as 200 km are permitted. The GAP plots associated with some of the paths considered for this paper can be seen in Fig. 3. (For comparison, the minimum V_∞ for a direct launch to Jupiter is 8.79 km/s.) In applying the GAP analysis, we note that for V_∞ greater than that giving the peak aphelion, it is better to use any extra ΔV for a deep-space maneuver, rather than for increased launch V_∞ . We also note that since these GAP plots only apply to ballistic trajectories, they cannot be used to analyze ΔV-EGA trajectories. (A detailed analysis of the ΔV-EGA is provided by Sims[24] and Sims et al.[25]) Another

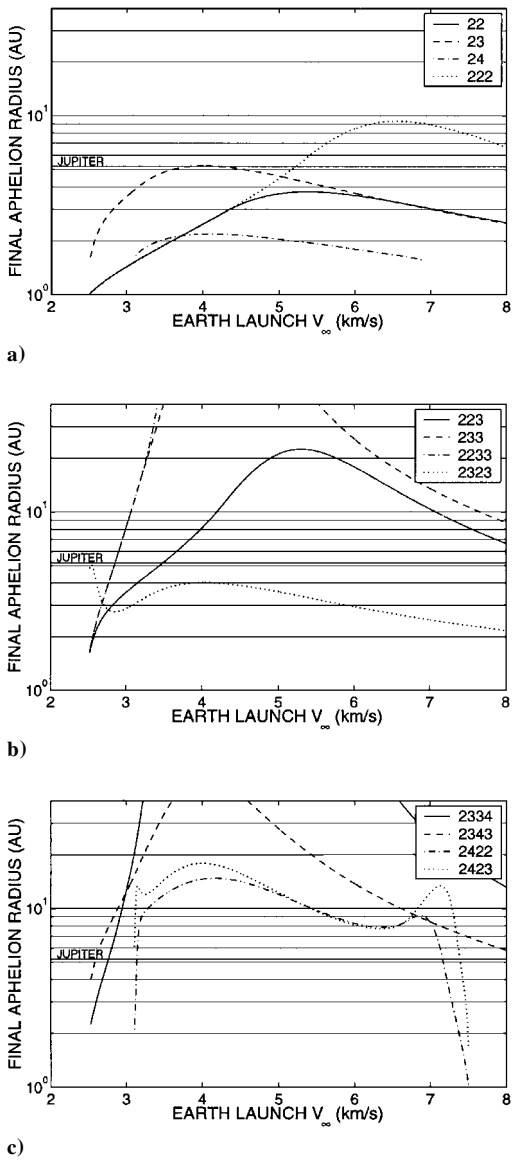

Fig. 3 GAP plots.

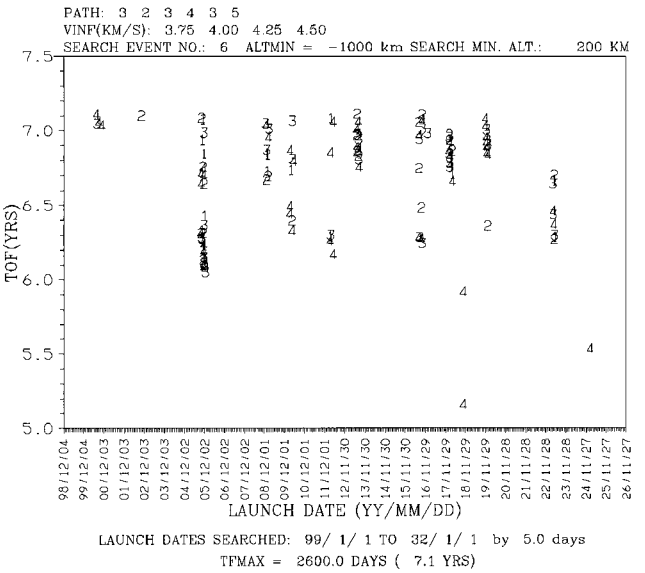

Fig. 4 VEME trajectories.

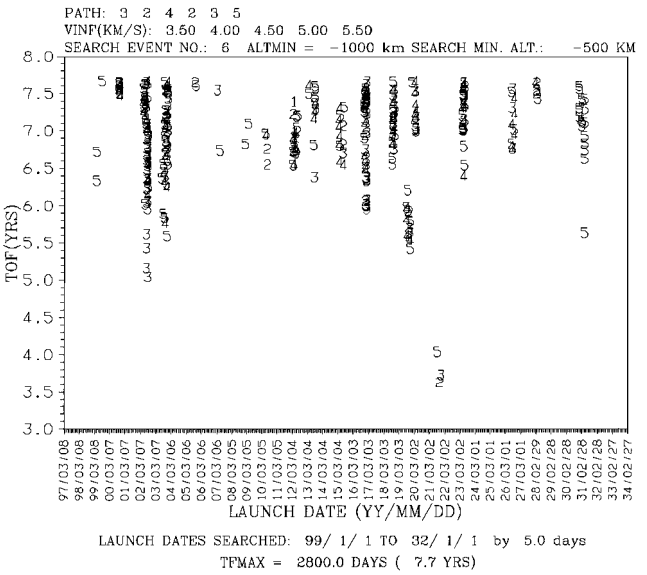

Fig. 5 VMVE trajectories.

point to make about these plots is that we assume the planets will always be in the right place at the right time (i.e., phasing issues are ignored). The GAP plots only indicate feasibility from an energy standpoint.

In Fig. 3 the GAP plots show some interesting characteristics for certain trajectory paths. (The paths in this figure are represented numerically; a VEE is denoted by 233.) The V^2 path (22 in Fig. 3a) and VM path (24 in Fig. 3a) show that, using these paths alone, it is impossible to get to Jupiter. It is generally true that the V^2 needs some deep-space ΔV to get to Jupiter. In the VM case STOUR confirms that there are no opportunities with flyby altitudes of 200 km or greater. The VEEGA, well known for its effectiveness, climbs through the Jupiter line at a V_∞ of 2.86 km/s and achieves very high aphelion distances for low launch V_∞ (Fig. 3b). The V^2E^2 (Fig. 3b) and the VE^2M (Fig. 3c) paths show great potential, both reaching Jupiter with launch V_∞ less than 3 km/s and achieving high aphelions. STOUR shows that the V^2E^2 is an effective trajectory. On the other hand, the VE^2M, although exhibiting tremendous potential, does not line up often. When the planets are aligned properly, however, the VE^2M can be a very efficient trajectory. Further validation of the GAP plots can be seen in Figs. 4 and 5. These figures are STOUR plots of the VEME and VMVE paths. The GAP plots predict that these paths should be able to reach Jupiter with low launch V_∞. The STOUR plots do, in fact, confirm this. An interesting characteristic of the VMVE plot is the very low TOF case in 2021 (i.e., 3.6 years). Also notable is that the path V^2E has a comparable TOF (about 3.7 years) in the same year. (VMVE is simply a V^2E that uses Mars as a leveraging body.) The planets align almost perfectly in this year.

From the GAP analysis we produce a rank-ordered list of paths that reach Jupiter. Thus Table 2 lists all 39 paths reaching Jupiter, ranked according to the lowest launch V_∞ needed. We note that the VEVE path has the lowest value (2.53 km/s). This table provides valuable insight in the process of pathfinding. The GAP analysis indicates that the first eight paths exhibit great potential as they can reach Jupiter with launch V_∞ of less than 3 km/s. However, some of these paths are unlikely to provide short TOFs because of multiple flybys with Earth or Mars. For example, the VEMM and VEEE can probably be rejected on this basis.

Selection of Candidate Paths

Because of the long computation time required to run all of the 120 flyby combinations in STOUR, we limited our search to a selected set of 25 paths, which are listed in Table 3. This selected set comprises all of the classical paths, and most of the nonclassical paths that appeared to be reasonable path candidates in terms of potential for short time of flight and low launch energy. The nonclassical path candidates are identified using the two approaches discussed in the preceding section (variations on classical paths and paths from the GAP analysis), in conjunction with engineering intuition regarding time of flight and orbit geometry. For example, the

Table 2 Rank order of paths to Jupiter based on GAP analysis

Rank	Path	V_∞, km/s[a]	Rank	Path	V_∞, km/s[a]	Rank	Path	V_∞, km/s[a]
1	VEVE	2.53	14	MEEM	3.15	27	MMM	4.17
2	VEME	2.60	15	VEM	3.16	28	VVMM	4.77
3	VEEM	2.76	16	VVEM	3.16	29	VVVM	4.93
4	VEMM	2.83	17	MEE	3.22	30	ME	4.95
5	VEE	2.86	18	MEEE	3.22	31	VVV	5.21
6	VVEE	2.86	19	MMEE	3.22	32	VVVV	5.21
7	VEEE	2.86	20	VVE	3.49	33	MMEM	5.31
8	MEVE	2.97	21	VVVE	3.49	34	MEVV	5.87
9	MEME	3.00	22	MEM	3.68	35	MME	6.08
10	VMEE	3.07	23	MMMM	3.74	36	MM	6.59
11	MEMM	3.07	24	VE	3.83	37	MMME	7.17
12	VMVE	3.11	25	VVME	3.94	38	VEMV	7.38
13	VMVV	3.14	26	VVMV	3.95	39	M	7.84

[a]Minimum launch V_∞ required.

Table 3 Best candidate(s) for each path (unoptimized)[a]

Path	Launch date YY-MM-DD	Launch V_∞, km/s	Flyby alt.,[b] km or ΔV,[b] km/s	Arrival V_∞, km/s	TOF, yr	Flyby times,[c] days after launch
E	04-02-24	5.21	0.875 (0)	6.54	4.1	678
E	14-03-03	5.22	0.585 (0)	5.81	6.7	1411
M	31-02-12	8.00		6.20	2.3	96
VV	31-08-06	5.00	0.376, 1.160 (1, 2)	7.04	4.2	178, 633
VV	31-08-14	5.00	1.493 (2)	7.24	4.5	174, r, 624
VE	05-10-01	4.50	0.179 (2)	6.38	5.1	416, 859
VE	15-07-06	4.00		7.62	6.2	177, 891
VM			No feasible trajectories			
MV			No feasible trajectories			
ME	12-08-05	5.50		5.60	5.0	640, 837
ME	26-11-15	6.00		8.94	3.9	145, 777
MM	18-05-19	7.00		5.42	6.3	78, r, 1452
VVV	01-04-22	6.00		7.21	6.3	397, 772, 1497
VVV	18-10-03	4.50	0.403 (2)	7.01	5.7	179, 581, 1289
VVE	20-03-08	4.00		6.03	5.9	103, 592, 1175
VVM	03-09-07	7.75	−964 (1)	6.60	5.5	408, r, 1082, 1180
VEV			No feasible trajectories			
VEE	29-11-05	3.25		6.40	5.6	146, 464, 1291
VEM	26-06-13	4.25	+183 (3)	5.75	5.2	431, 871, 1007
VMV	05-10-31	5.50	−266, −604 (1, 3)	7.13	6.6	404, 834, 1479
MVM			No feasible trajectories			
MEE	00-12-21	5.00		8.06	7.0	746, 1127, r, 1858
VVEE	18-09-17	3.50		7.09	6.8	159, r, 609, 1041, r, 1772
VVMV	18-10-24	5.00		6.98	5.9	175, 570, 667, 1278
VEVE	26-08-27	3.50		8.27	6.3	176, 695, 1043, 1590
VEEM	26-08-09	3.00		7.34	6.5	105, 577, r, 1672, 1748
VEME	23-05-30	3.25		5.58	6.4	146, 461, 623, 1276
VMVV	12-04-27	4.00		7.12	7.0	181, 799, 1101, 1708
VMVE	21-10-27	4.00	−346 (4)	7.32	3.6	148, 275, 608, 663
VMVMV	17-01-06	4.50	+160 (1)	7.02	7.0	136, 800, 994, 1558, 1665

[a]The 25 paths listed here are referred to as the selected set, as discussed in the text.
[b]Only flyby altitudes below 200 km are listed; they are prefixed with a + or − sign. The parenthetical numbers indicate the associated flyby number. Deep-space ΔV, if present, are listed without a prefixed sign; the parenthetical numbers indicate the flyby number preceding the maneuver, with 0 signifying Earth launch.
[c]An "r" between the flyby times indicates that resonance occurs on that leg.

GAP plots indicate that M^2, V^3, and VE^2 all reach Jupiter; however, adding an extra encounter of the last flyby body would probably have little effect on the launch energy, while making the time of flight prohibitively long. Thus there is no need to study M^3, V^4, and VE^3. Other paths, such as M^2E, are unattractive because the double Mars encounter, when best used, raises perihelion above Earth's orbit, thus eliminating all paths starting with M^2E. Also, one five-flyby path, VMVMV, is considered because of its dramatic potential for two leveraging-effect gravity assists. Finally, it should be noted that Table 3 does not contain all reasonable nonclassical types, for example, V^3E, V^3M, and MEM are missing. These and other paths were rejected because they were deemed less likely to produce many viable results with acceptable TOFs, and because of the time-intensive searches involved. For the same reason, an assessment of leveraging with STOUR was made only for the V^2, V^3, VEEGA, and ΔV-EGA trajectories of Table 3.

Results

The paths in the selected set were first examined over the whole launch period (1 January 1999–31 December 2031) using STOUR. To present this enormous set of data, we divide the paths into two groups, depending on whether Earth is used as a flyby body. (In missions utilizing radioisotope power sources, we can reduce the risk of Earth impact by not using Earth as a gravity-assist body.) For each group we list up to three of the most attractive trajectories in each calendar year (Tables 4 and 5). In making our selections for each year, we sought low TOF with 1) low deep-space ΔV (or above-surface flybys), 2) low launch V_∞, and 3) low arrival V_∞. Of course, some sort of trade was typically involved between these quantities. As a rough rule of thumb, of these three quantities, low deep-space ΔV was considered the most important and low arrival V_∞ the least important. Approximately speaking, an extra 0.5–1 km/s in launch V_∞, or up to 0.5 km/s in deep-space ΔV, would be accepted only

Table 4 Promising trajectories including Earth flybys (unoptimized), listed by date

Path	Launch date YY-MM-DD	Launch V_∞, km/s	Flyby alt.,[a] km or ΔV,[a] km/s	Arrival V_∞, km/s	TOF, yr	Flyby times,[b] days after launch
VE	99-03-27	4.50	0.314 (2)	5.79	5.1	339, 947
VEE	99-05-21	3.00	0.395 (2)	5.90	5.8	155, 438, 1259
VEE	99-06-25	3.75		5.77	7.0	178, 492, r, 1588
VEE	00-08-23	3.50	0.070 (2)	6.53	6.6	374, 754, 1590
VEE	01-02-24	3.75		5.82	6.6	173, 693, r, 1424
VEE	02-07-15	3.50		6.07	5.9	145, 633, 1256
VEE	03-11-07	4.00		6.62	6.5	383, 776, 1623
VE	04-05-04	4.50	0.794 (2)	5.97	4.4	140, 652
VEE	04-06-17	5.00		6.55	6.0	155, 680, r, 1410
VEE	05-10-12	3.50		6.65	5.6	162, 476, 1300
VE	06-12-10	4.50	0.868 (2)	6.32	5.1	433, 835
VEE	07-02-24	4.00		6.56	6.5	359, 772, 1631
VEE	08-12-09	4.00		6.71	5.7	152, 634, r, 1365
VEE	09-01-24	3.75		5.60	6.1	167, 484, 1315
VEME	10-04-18	4.00		8.27	6.4	365, 936, 1512, 1680
VEE	10-07-17	3.00	0.431 (2)	6.21	6.6	133, 753, 1568
VEE	11-09-20	4.25		5.99	7.6	416, 777, r, 1508
VEE	12-04-13	3.50		5.88	6.1	181, 498, 1329
VEE	13-10-29	4.00		5.68	6.0	91, 401, r, 1131
VEE	14-11-23	4.00		7.16	7.3	442, 825, r, 1921
VEVE	14-11-28	4.50		8.49	7.0	439, 999, 1289, 1880
VEE	15-05-27	3.75		6.74	5.9	148, 655, r, 1386
VE	16-09-18	4.50	0.255 (2)	6.20	5.1	349, 924
VEE	17-01-06	3.75		6.64	6.5	134, 448, r, 1179
VE	18-07-25	4.50	−377, −40 (1, 2)	8.58	4.5	421, 1051
VEE	18-09-08	3.50		6.03	6.6	160, 679, r, 1410
VMVE	19-10-23	4.00	−172 (4)	7.43	5.6	433, 1024, 1350, 1400
VEE	20-03-26	3.00		6.75	6.4	171, 506, r, 1601
VEE	20-04-05	3.50		6.22	5.4	156, 455, r, 1186
VMVE	21-10-27	4.00	−346 (4)	7.32	3.6	148, 275, 608, 663
VVEE	21-11-13	3.50		6.86	7.1	173, 616, 1087, r, 1818
VVE	22-01-20	5.00		6.68	5.9	171, 563, 1390
VEME	23-05-30	3.25		5.58	6.4	146, 461, 623, 1276
VEE	24-08-28	3.50		6.08	6.8	371, 942, 1538
VEE	25-02-23	4.00		6.60	6.1	177, 699, r, 1429
VEM	26-06-13	4.25	+183 (3)	5.75	5.2	431, 871, 1007
VEEM	26-08-09	3.00		7.34	6.5	105, 577, r, 1672, 1748
VE	27-10-16	5.00	−124 (2)	6.09	4.8	390, 792
VEE	28-03-09	3.50	0.697 (2)	6.09	6.6	121, 746, 1460
VE	28-03-19	4.50	0.699 (2)	6.05	4.6	201, 712
VEE	29-11-05	3.25		6.40	5.6	146, 464, 1291
VEVE	30-12-24	4.50		7.63	6.3	422, 824, 913, 1607
VEE	31-04-23	3.25	0.674 (2)	6.81	6.2	170, 817, 1529
VE	31-07-17	4.50	0.690 (2)	6.39	4.1	180, 701

[a]Only flyby altitudes below 200 km are listed; they are prefixed with a + or − sign. The parenthetical numbers indicate the associated flyby number. Deep-space ΔV, if present, are listed without a prefixed sign; the parenthetical numbers indicate the flyby number preceding the maneuver.
[b]An "r" between the flyby times indicates that resonance occurs on that leg.

if it reduced TOF by at least a year. At the other end of the spectrum, increases of 0.5–2 km/s in arrival V_∞ would be accepted even if TOF was decreased by only 0.5–1 year. Sometimes, especially when these quantities changed simultaneously, rather than choosing between several good candidates, up to three were listed, as for the year 1999 in Table 4, or 2031 in Table 5. A similar selection approach was taken in evaluating the best that each path had to offer over the whole launch period. These unoptimized trajectories are shown in Table 3. We note that each trajectory listed in the tables is typically a member of a trajectory family that can show significant variation in the key quantities near the same launch date. Thus, for example, mission designers wanting to use Jupiter as a gravity-assist body for exploration of the outer solar system should usually be able to find similar trajectories to those listed, but with higher arrival V_∞.

Table 6 shows ΔV-optimized versions of the Tables 4 and 5 trajectories up to 2010, along with several noteworthy trajectories after 2010. The optimization (performed using MIDAS[22]) sought the minimum sum of launch ΔV and deep-space ΔV. (Flyby times and other data are listed in these tables to facilitate re-creation of the trajectories.) A comparison of the optimized with the unoptimized trajectories demonstrates the relatively close correspondence between the two. One factor that affects this correspondence is the granularity of the search in STOUR: the size of the increments in launch V_∞ and launch date. The latter was always taken as five days, whereas the former was typically 0.25 km/s (e.g., for the VEEGAs) or 0.5 km/s (e.g., for the V^3s), although 1 km/s was used for some of the less interesting paths, such as V^2M. (These increments represent a relatively fine search grid over the continuum of trajectories.) In some cases, particularly those involving leveraging, the optimized solution was considerably better than the unoptimized, due to the fact that STOUR does not try to optimize the leveraging maneuver for each specific trajectory; STOUR merely shows that a feasible leveraging family exists at a particular time.

It is immediately obvious that the classical VEEGAs, VEGAs, and V^3s dominate the trajectory tables, indicating that the attention given to these trajectories by other researchers, such as Diehl and Myers,[15] was well placed. A somewhat surprising result is that the well-known ΔV-EGA does not perform well enough to appear in Table 4. Another general observation is that the best trajectories involving Earth flybys are significantly better than the best of the no-Earth-flyby trajectories, by almost any performance measure, again corresponding well with the choice by Diehl and Myers to examine only VEGAs and VEEGAs.

Table 5 Promising trajectories without Earth flybys (unoptimized), listed by date

Path	Launch date YY-MM-DD	Launch V_∞, km/s	Flyby alt.,[a] km or ΔV,[a] km/s	Arrival V_∞, km/s	TOF, yr	Flyby times,[b] days after launch
VMVV	99-04-26	5.50		6.49	6.7	322, 616, 850, r, 1524
VVV	00-08-23	4.50	1.17 (1)	6.99	6.3	365, 860, 1478
VVV	01-02-24	4.50	0.145, 0.230 (1, 2)	7.33	6.4	187, 638, 1548
VVV	01-04-22	6.00		7.21	6.3	397, 772, 1497
VVV	02-08-23	6.00	+177, +17 (1, 3)	7.60	5.5	70, r, 519, 1246
VMVV	03-11-26	4.00		8.15	7.2	370, 715, 1243, 1974
VVV	04-07-15	6.00		7.18	6.9	168, r, 617, r, 1741
VVV	05-10-31	4.50	0.519, 0.039 (2, 3)	7.16	5.6	85, 580, 1270
VVV	06-01-29	7.00	−280 (3)	6.82	6.9	382, 963, r, 1637
VVMV	07-04-14	5.00		7.07	6.9	324, r, 774, 895, 1433
VVV	07-10-27	6.50		7.52	6.0	142, r, 592, r, 1491
VVV	08-12-04	4.50	0.338, 0.683 (1, 2)	7.11	7.1	435, 893, 1812
VVV	09-02-12	4.50	1.004, 0.554 (2, 3)	7.38	7.0	189, 595, 1246
VVV	10-05-18	4.50	0.791, 0.278, 0.452 (1, 2, 3)	7.15	6.2	347, 786, 1510
VVV	11-01-15	6.50	−551 (1)	7.28	6.2	154, r, 603, r, 1502
VMVV	12-04-27	4.00		7.12	7.0	181, 799, 1101, 1708
VVV	13-09-04	6.50		7.37	6.8	327, r, 776, 1718
VVV	14-04-09	7.00	−394, −366 (1, 3)	8.98	5.2	143, r, 593, r, 1267
VVV	15-07-29	6.50		8.94	6.4	418, 792, 1733
VVV	15-08-10	4.50	0.617 (2)	7.27	6.7	172, 567, 1502
VVV	16-12-27	6.00	+177 (3)	8.18	6.4	304, r, 753, 1689
VMVMV	17-01-06	4.50	+160 (1)	7.02	7.0	136, 800, 994, 1558, 1665
VVV	18-10-03	4.50	0.403 (2)	7.01	5.7	179, 581, 1289
VVMV	18-10-24	5.00		6.98	5.9	175, 570, 667, 1278
VVV	19-01-11	6.50		6.86	6.1	155, 728, r, 1402
VVV	20-03-16	6.00	+39 (1)	8.46	5.8	79, r, 529, 1470
VVV	21-11-26	4.50	0.338, 0.522, 0.649 (1, 2, 3)	7.16	5.7	184, 643, 1331
VVV	22-03-14	6.50	+33 (1)	7.06	6.8	376, 748, 1692
VVV	22-12-26	4.50	0.292, 0.491, 0.304 (1, 2, 3)	6.53	6.9	478, 945, 1641
VVV	23-05-25	5.50		6.97	6.9	83, 596, r, 1720
VVV	24-08-17	4.50	0.857, 0.390, 0.043 (1, 2, 3)	7.46	6.2	365, 797, 1511
VVV	25-03-20	4.50	0.138, 0.244 (1, 2)	7.14	6.4	173, 624, 1531
VVV	25-05-12	6.00		10.50	5.6	160, 535, 1476
VMVV	26-08-07	4.50		7.11	7.2	419, 515, 795, 1748
VMVV	26-08-07	4.50	−34 (4)	7.45	6.2	419, 515, 795, r, 1469
M	27-02-08	8.00		5.87	6.5	1563
VVV	27-11-30	4.50	0.230, 1.097, 0.176 (1, 2, 3)	7.27	6.7	353, 833, 1473
VVV	28-07-15	6.00		7.32	6.9	165, r, 614, r, 1513
VVV	29-10-15	4.50	0.396 (2)	7.12	6.2	414, 815, 1524
VVV	30-12-19	4.50	0.453, 0.893 (1, 2)	8.64	6.0	399, 884, 1579
M	31-02-12	8.00		6.20	2.3	96
VMVV	31-04-23	5.50	+142 (4)	7.33	7.2	317, 528, 755, r, 1429

[a]Only flyby altitudes below 200 km are listed; they are prefixed with a + or − sign. The parenthetical numbers indicate the associated flyby number. Deep-space ΔV, if present, are listed without a prefixed sign; the parenthetical numbers indicate the flyby number preceding the maneuver.
[b]An "r" between the flyby times indicates that resonance occurs on that leg.

The classical trajectories exhibit some unexpected resonance characteristics. (Sequential encounters of the same body are said to exhibit resonance, or equivalently are said to be resonant, if the time between the encounters is an integer multiple of the body's orbital period.) Whereas most of the VEEGAs have around two years between Earth flybys as expected, the 99-06-25 and 14-11-23 cases of Table 4 exhibit a three-year resonance. Roughly half of the V^3s in Table 5, resonant and nonresonant, have about two Venus years between the first two Venus flybys, and about four between the last two, which we denote by [∼2; ∼4]. Roughly half are [∼2; ∼3]. Two trajectories, in 2004 and 2023, manage to achieve a five-Venus-year resonance. Surprisingly, there are two instances of a [∼3; =3], where the equal sign denotes an exact resonance, in 2006 and 2019; these are among the worst of the listed V^3s. In contrast, the V^3s listed in Table 3 are both [∼2; ∼3], due to their slightly shorter flight times.

In spite of the success of the classical paths, the nonclassical paths can 1) occasionally provide advantages even over the best classical trajectory, 2) sometimes improve on a classical trajectory in the same year, and 3) provide trajectories in years in which no viable classical trajectories exist. The first point is exemplified by the 2021 VMVE trajectory shown in Tables 4 and 6. The flight time of this VMVE is not even one year greater than that of a classical Hohmann transfer, while the launch V_∞ is less than half that of the Hohmann, and only minimal deep-space ΔV is needed. An instance of the second point is the 2023 VEME (Tables 3, 4, and 6), whose launch V_∞ is 0.5 km/s less than the nearest VEEGA competitor, and whose TOF is also somewhat less. Similarly, the VMV^2 in 2012 (Tables 3 and 5) is significantly better than any 2012 V^3. An example of the third point is the V^2E in 2022 (Table 4), a year in which there are no VEGAs or VEEGAs of the typical sort. [The only comparable VEEGA in 2022 has similar launch energy (uncharacteristically high for a VEEGA) but slightly higher arrival V_∞ and TOF.]

It is interesting to note that although Mars can be frequently used as a leveraging body for the VEEGAs (Fig. 4), using Mars seldom improves performance, as witnessed by the dearth of VEME trajectories in Table 4. On the other hand, Mars is much less often available as a leveraging body with the V^3s, but when it is available, it is very efficacious (Table 5). Also, it is seen that VMV^2 trajectories are more effective than V^2MV. One reason for this is that with the VMV^2 there are two Venus flybys available to turn the increased V_∞, rather than just one. Mars need not always be used as a leveraging body. For example, Mars can be used in 2031 to improve on the classical Hohmann transfer, in terms of both TOF and launch energy.

Last, we note that for many of the nonclassical paths, the optimal relative alignment of the planets does not recur often. The Mars gravity assist recurs every 47–49 years. The remarkable 2021 VMVE repeats in similar form about every 45 years, although a slight shift occurs after the beginning of the 22nd century. For this path the relative orientations of 2021 are sometimes not repeated as precisely as those of the 2031 Mars gravity assist. This difference

Table 6 ΔV-optimized trajectories, listed by date within each group

Path	Launch date YY-MM-DD	Launch V_∞, km/s	Deep-space ΔV, km/s	Arrival V_∞, km/s	TOF, yr	Flyby times,[a] days after launch
			Trajectories with Earth flybys, 1999–2010			
VE	99-03-27	4.50	0.298	5.80	5.1	339, 947
VEE	99-05-16	3.03	0.276	6.10	5.8	157, 438, 1257
VEE	99-06-09	3.37	0	5.55	7.3	175, 513, r, 1608
VEE	00-08-11	3.07	0	6.55	6.6	387, 766, 1604
VEE	01-02-24	3.75	0	5.82	6.6	173, 693, r, 1423
VEE	02-07-23	3.40	0	6.56	5.7	140, 624, 1247
VEE	03-11-19	3.80	0	6.62	6.5	373, 764, 1610
VEE	04-03-12	3.56	0.471	6.36	6.3	122, 740, r, 1470
VE	04-04-23	4.14	0.719	6.03	4.3	145, 663
VEE	05-10-28	3.14	0	6.65	5.6	153, 458, 1282
VE	06-12-16	4.05	0.813	6.20	4.9	429, 822
VEE	07-02-28	3.93	0	6.56	6.5	355, 768, 1626
VEE	08-12-09	4.02	0	6.70	5.7	152, 634, r, 1364
VEE	09-01-21	3.68	0	5.50	6.3	172, 488, 1320
VEME	10-04-06	3.69	0	8.27	6.4	377, 947, 1523, 1692
VEE	10-07-21	2.94	0.360	6.21	6.6	129, 747, 1560
			Trajectories without Earth flybys, 1999–2010			
VMVV	99-04-27	5.46	0	6.49	6.7	320, 615, 848, r, 1522
VVV	00-08-04	2.97	0.734	6.62	6.6	393, 825, 1523
VVV	01-03-04	3.89	0.360	7.33	6.4	173, r, 628, r, 1539
VVV	01-04-24	5.93	0	7.24	6.3	394, 770, 1494
VVV	02-08-25	4.54	0.438	7.92	5.4	77, 527, 1244
VMVV	03-12-01	3.94	0	8.05	7.2	365, 710, 1237, 1968
VVV	04-07-09	5.34	0.037	8.60	6.5	162, r, 611, r, 1737
VVV	05-10-30	4.20	0.508	7.45	6.3	89, 576, 1278
VVV	06-01-04	5.34	0.171	6.83	7.0	403, 991, r, 1660
VVMV	07-04-09	4.87	0	7.06	6.9	329, r, 779, 900, 1438
VVV	07-10-10	5.78	0.011	8.36	5.9	155, r, 605, r, 1503
VVV	08-12-01	4.26	0.608	7.56	6.9	430, r, 888, r, 1805
VVV	09-02-21	3.77	1.044	7.36	7.0	173, 565, r, 1240
VVV	10-05-19	4.28	1.098	6.42	7.0	349, 837, 1483
			Notable trajectories, 2011–2031			
VVMV	18-11-02	4.67	0	7.05	6.1	164, 563, 660, 1267
VMVE	21-10-27	3.99	0.425	6.90	3.7	148, 275, 607
VEME	23-05-28	3.25	0	5.58	6.4	147, 463, 624, 1278
VEEM	26-08-03	2.93	0	7.34	6.6	110, 582, r, 1678, 1753
M	31-02-15	7.84	0	5.83	2.5	95

[a]An "r" between the flyby times indicates that resonance occurs on that leg.

in the precision with which the relative orientations recur might be expected, since the VMVE requires the realignment of four planets, not just three, whose periods are not in simple ratios to each other.

Conclusions

We have taken a systematic approach to the identification of low-energy, gravity-assist trajectories to Jupiter with launch opportunities in the next three decades. Starting from a list of all possible combinations of up to four flybys with Venus, Earth, and Mars, we used energy considerations, estimates of time of flight, and engineering judgment to reduce the number of paths to a selected set of 25 cases. We then employed an automated design program to calculate all occurrences of each path for the 33-year launch period. We also identified the ΔV-optimal paths for the first decade and selected years thereafter. We found that classical trajectories, such as the Venus–Earth–Earth gravity assist, are likely to be the trajectories of choice in any given year; however, nonclassical trajectories, such as the Venus–Mars–Venus–Earth in 2021, can sometimes offer significant advantages at little cost.

Although we make no claim that these are global optimal solutions, we believe that our results are broadly representative of the effectiveness of both classical and nonclassical trajectory paths. Our methods of pathfinding and automated trajectory design should be applicable in the search for gravity-assist trajectories to other solar system bodies. We hope our trajectories to Jupiter will provide designers with useful benchmarks for future missions to our largest planet.

Acknowledgments

This research has been supported in part by the Jet Propulsion Laboratory, California Institute of Technology, under Contract 961211. We are grateful to Dennis V. Byrnes (Technical Manager), Jan M. Ludwinski, and Robert W. Maddock for providing useful information, guidance, and helpful suggestions. We also thank Nathan J. Strange, a graduate student in the School of Aeronautics and Astronautics at Purdue University, for his assistance.

References

[1]Broucke, R. A., "The Celestial Mechanics of Gravity Assist," AIAA Paper 88-4220, Aug. 1988.

[2]Battin, R. H., *An Introduction to the Mathematics and Methods of Astrodynamics*, 1st ed., AIAA, New York, 1987, pp. 423, 424.

[3]Battin, R. H., "The Determination of Round-Trip Planetary Reconnaissance Trajectories," *Journal of the Aero/Space Sciences*, Vol. 26, No. 9, 1959, pp. 545–567.

[4]Sedov, L. I., "Orbits of Cosmic Rockets Toward the Moon," *ARS Journal*, Vol. 30, No. 1, 1960, pp. 14–21.

[5]Deerwester, J. M., "Jupiter Swingby Missions to the Outer Planets," *Journal of Spacecraft and Rockets*, Vol. 3, No. 10, 1966, pp. 1564–1567.

[6]Flandro, G. A., "Fast Reconnaissance Missions to the Outer Solar System Utilizing Energy Derived from the Gravitational Field of Jupiter," *Astronautica Acta*, Vol. 12, No. 4, 1966, pp. 329–337.

[7]Gillespie, R. W., Ragsac, R. V., and Ross, S. E., "Prospects for Early Manned Interplanetary Flights," *Astronautics and Aerospace Engineering*, Vol. 1, No. 7, 1963, pp. 16–21.

[8]Hollister, W. M., "Mars Transfer via Venus," AIAA Paper 64-647, Aug. 1964.

[9]Minovitch, M. A., "The Determination and Characteristics of Ballistic Interplanetary Trajectories Under the Influence of Multiple Planetary Attractions," Jet Propulsion Lab., TR 32-464, California Inst. of Technology, Pasadena, CA, Oct. 1963.

[10]Niehoff, J. C., "Gravity-Assisted Trajectories to Solar System Targets," *Journal of Spacecraft and Rockets*, Vol. 3, No. 9, 1966, pp. 1351–1356.

[11]Ross, S. E., "Trajectory Design for Planetary Mission Analysis," *Recent Developments in Space Flight Mechanics*, Vol. 9, edited by P. B.

Richards, Science and Technology Series, American Astronautical Society, Washington, DC, 1966, pp. 3–43.

[12]Sohn, R. L., "Venus Swingby Mode for Manned Mars Missions," *Journal of Spacecraft and Rockets*, Vol. 1, No. 5, 1964, pp. 565–567.

[13]Sturms, F. M., and Cutting, E., "Trajectory Analysis of a 1970 Mission to Mercury via a Close Encounter with Venus," AIAA Paper 65-90, Jan. 1965.

[14]Stancati, M. L., Friedlander, A. L., and Bender, D. B., "Launch Opportunity Classification of VEGA and ΔV-EGA Trajectories to the Outer Planets," AIAA Paper 76-797, Aug. 1976.

[15]Diehl, R. E., and Myers, M. R., "Gravity-Assist Trajectories to the Outer Solar System," Jet Propulsion Lab., JPL Publication D-4677, California Inst. of Technology, Pasadena, CA, Sept. 1987.

[16]Williams, S. N., "Automated Design of Multiple Encounter Gravity-Assist Trajectories," M.S. Thesis, School of Aeronautics and Astronautics, Purdue Univ., West Lafayette, IN, Aug. 1990.

[17]Longuski, J. M., and Williams, S. N., "Automated Design of Gravity-Assist Trajectories to Mars and the Outer Planets," *Celestial Mechanics and Dynamical Astronomy*, Vol. 52, No. 3, 1991, pp. 207–220.

[18]Rinderle, E. A., "Galileo User's Guide, Mission Design System, Satellite Tour Analysis and Design Subsystem," Jet Propulsion Lab., JPL Publication D-263, California Inst. of Technology, Pasadena, CA, July 1986.

[19]Patel, M. R., "Automated Design of Delta-V Gravity-Assist Trajectories for Solar System Exploration," M.S. Thesis, School of Aeronautics and Astronautics, Purdue Univ., West Lafayette, IN, Aug. 1990.

[20]Patel, M. R., and Longuski, J. M., "Automated Design of Delta-V Gravity-Assist Trajectories for Solar System Exploration," American Astronautical Society, AAS Paper 93-682, Aug. 1993.

[21]Staugler, A. J., "STOUR (Satellite Tour Design Program) User's Guide for the ΔV-EGA and V_∞ -Leveraging Routines," School of Aeronautics and Astronautics, TR, Purdue Univ., West Lafayette, IN, June 1996.

[22]Sauer, C. G., "MIDAS: Mission Design and Analysis Software for the Optimization of Ballistic Interplanetary Trajectories," *Journal of the Astronautical Sciences*, Vol. 37, No. 3, 1989, pp. 251–259.

[23]Hollenbeck, G. R., "New Flight Techniques for Outer Planet Missions," American Astronautical Society, AAS Paper 75-087, July 1975.

[24]Sims, J. A., "Delta-V Gravity-Assist Trajectory Design: Theory and Practice," Ph.D. Dissertation, School of Aeronautics and Astronautics, Purdue Univ., West Lafayette, IN, Dec. 1996.

[25]Sims, J. A., Longuski, J. M., and Staugler, A. J., "V_∞ Leveraging for Interplanetary Missions: Multiple-Revolution Orbit Techniques," *Journal of Guidance, Control, and Dynamics*, Vol. 20, No. 3, 1997, pp. 409–415.

F. H. Lutze Jr.
Associate Editor